Title

α-Toxin Regulates Local Granulocyte Expansion from Hematopoietic Stem and Progenitor Cells in Staphylococcus aureus–Infected Wounds

Journal

The Journal of Immunology, 199(5)

ISSN

0022-1767

Authors

Falahee, Patrick C
Anderson, Leif S
Reynolds, Mack B
et al.

Publication Date

2017-09-01

DOI

10.4049/jimmunol.1700649

Peer reviewed

HHS Public Access

Author manuscript

J Immunol. Author manuscript; available in PMC 2018 September 01.

Published in final edited form as:

J Immunol. 2017 September 01; 199(5): 1772–1782. doi:10.4049/jimmunol.1700649.

Alpha-toxin regulates local granulocyte expansion from hematopoietic stem and progenitor cells in *Staphylococcus aureus*-infected wounds

Patrick C. Falahee[*,1], **Leif S. Anderson**[*,1], **Mack B. Reynolds**[*], **Mauricio Pirir**[*], **Bridget E. McLaughlin**[†], **Carly A. Dillen**[§], **Ambrose L. Cheung**[‡], **Lloyd S. Miller**[§], and **Scott I. Simon**[*]

[*]Department of Biomedical Engineering, University of California Davis, Davis, CA

[†]Comprehensive Cancer Center Flow Cytometry Shared Resource, University of California Davis, Davis, CA

[‡]Department of Microbiology and Immunology, Geisel School of Medicine at Dartmouth, Hanover, NH

[§]Department of Dermatology, The Johns Hopkins University School of Medicine, Baltimore, MD

Abstract

The immune response to *Staphylococcus aureus* infection in skin involves the recruitment of neutrophils (PMN) from the bone marrow via the circulation and local granulopoiesis from hematopoietic stem and progenitor cells (HSPC) that also traffic to infected skin wounds. We focus on regulation of PMN number and function and the role of pore-forming alpha-toxin (AT), a virulence factor that causes host cell lysis and elicits inflammasome-mediated IL-1β secretion in wounds. Infection with wild type *S. aureus* enriched in AT reduced PMN recruitment and resulted in sustained bacterial burden and delayed wound healing. In contrast, PMN recruitment to wounds infected with an isogenic AT mutant strain (ΔAT) was unimpeded, exhibiting efficient bacterial clearance and hastened wound resolution. HSPC recruited to infected wounds was unaffected by AT production and were activated to expand PMN numbers in proportion to *S. aureus* abundance in a manner regulated by TLR2 and IL-1 receptor signaling. Immunodeficient MyD88 knockout mice infected with *S. aureus* experienced lethal sepsis that was reversed by PMN expansion mediated by injection of wild type HSPC directly into wounds. We conclude that AT induced IL-1β promotes local granulopoiesis and effective resolution of *S. aureus*-infected wounds, revealing a potential antibiotic free strategy for tuning the innate immune response to treat *MRSA* infection in immunodeficient patients.

Address correspondence and request reprints to Dr. Scott I. Simon, Department of Biomedical Engineering, University of California, Davis, 451 E. Health Sciences Drive, Davis, CA 95616. sisimon@ucdavis.edu. Phone: 530-752-0299.

[1]P.C.F. and L.S.A. made equal contributions to this manuscript.

Authorship

Contribution: P.C.F. and L.S.A. provided equal contributions to the design and performance of this work, data analysis and writing of the manuscript. M.B.R., M.P., and B.E.M. performed the research and analyzed data. A.L.C. designed the research, interpreted the data and wrote the manuscript. L.S.M. designed the research, interpreted the data and wrote the manuscript. S.I.S. designed the research, interpreted the data and wrote the manuscript.

Conflict-of-interest disclosure: The authors declare no competing financial interests.

Introduction

Staphylococcus aureus infection of acute and chronic wounds is a major complication associated with delayed wound healing(1). These infections are caused by virulent and multi-drug resistant strains, including community-acquired methicillin-resistant *S. aureus* (*MRSA*) isolates such as USA300(2). The neutrophilic response is critical to controlling *S. aureus* infections, as invasive infections commonly occur in individuals with congenital and acquired defects in neutrophil number or function(3). The innate immune response to *S. aureus* includes robust and sustained recruitment of mature neutrophils (PMN) from the bloodstream to the site of infection(4). Recently, we discovered a novel mechanism for augmenting PMN numbers involving recruitment of hematopoietic stem and progenitor cells (HSPC) that also traffic to *S. aureus*-infected wounds and undergo local granulopoiesis in proportion to bacterial burden. We demonstrated that local granulopoiesis requires TLR2/MyD88 signaling and that depletion of circulating HSPC is lethal for infected mice (5, 6). Given the importance of local granulopoiesis in combating *S. aureus*, additional studies are warranted to better understand the mechanisms regulating HSPC trafficking and production of PMN at the site of infection.

S. aureus produces a variety of virulence factors that counteract neutrophil recruitment and antimicrobial function(7–10). With particular relevance to skin infections, *S. aureus* produces alpha-toxin (AT; also known as α-hemolysin) a pore-forming toxin that lyses host cells(11) and contributes to disease severity(12–15). AT directly lyses perivascular macrophages in the skin, leading to defective and delayed PMN extravasation(16). Neutralizing AT with a high affinity anti-AT mAb has been shown to be an effective therapy to reduce disease severity by restoring recruitment of neutrophils and T cells to the infected skin and decreasing dermonecrosis (3). However, whether AT plays an additional role in regulating HSPC recruitment and local granulopoiesis during a *S. aureus* wound infection is unknown. In the current study, we set out to determine whether AT contributes to the dynamics of neutrophil numbers in a *S. aureus*-infected skin wound by impacting HSPC trafficking and local granulopoiesis, which would provide novel insights into the mechanisms that govern local granulopoiesis during a *S. aureus* skin wound infection.

We employed a transgenic mouse model of cutaneous infection that facilitates noninvasive quantification of PMN kinetics by whole animal fluorescence imaging of Lys-M-EGFP recruited into a full-thickness skin wound. Following inoculation with wild-type *S. aureus* versus an isogenic AT-deficient mutant (ΔAT), we observed a significant attenuation in the recruitment of PMN from the peripheral blood to wounds inoculated with *S. aureus* as compared to ΔAT, despite a 10-fold higher abundance of wild-type colonization in the wound. HSPC trafficked to the site of infection with equal efficiency following inoculation with either strain, signifying that progenitor cell trafficking is sensitive to wounding and infection but not AT-mediated toxicity. Further, we show that fortifying wounds by direct injection of HSPC that undergo local myeloid expansion can rescue an immunodeficient host from lethal infection with *S. aureus*. These data demonstrate the critical role of IL-1 and TLR2 signaling of HSPC granulopoiesis in protecting the host from virulent *S. aureus* and demonstrate a novel cell therapy approach for treatment of AT producing *S. aureus* infections.

Materials & Methods

Staphylococcus aureus strains and growth conditions

S. aureus strains used in this study were derivatives of SH1000 that produce high levels of lytic AT(18). The *hla* mutant of SH1000 (designated as ΔAT) was constructed by transducing the mutation from *S. aureus* strain ALC837 (RN6390 with *hla::ermC*), using phage Φ11. Transductants were screened by PCR with flanking *hla*-specific primers as well as outside primers. The putative *hla* mutant of SH1000 was then confirmed by sequencing the PCR fragment containing the mutation and flanking sequences. The *hla* complement, ALC2801, was created by transducing pCL84::*hla (*hla inserted into the lipase gene) from *S. aureus* 8325-4 into ALC2801 using phage phi 11. Transductants were selected on TSA with tet 3 ug/ml and verified by the absence of lipase on egg yolk agar. Successful transformants were verified by restoration of hemolysis on Sheep blood agar plate and confirmed by PCR following by sequencing. In some experiments, we utilized the bioluminescent strain ALC2906 (designated as S. aureus lux), which possesses the shuttle plasmid pSK236 with the pbp2 (penicillin-binding protein 2) promoter fused to the luxABCDE cassette from Photorhabdus luminescencs, as previously described(19). All SH1000 strains and mutants were cultured as described previously(5, 6).

Mice

Mice used in this study were on a C57BL/6 genetic background and between 8 to 16 weeks old. C57BL/6J (wild-type), B6.SJL-Ptprc^{a} Pepc^{b}/BoyJ (CD45.1), and B6.129P2(SJL)-Myd88$^{tm1.1Defr}$/J (MyD88$^{-/-}$) mice were purchased from Jackson Labs. LysM-EGFP and MyD88$^{-/-}$ × LysM-EGFP transgenic mice were bred in animal facilities at the University of California Davis. IL-1β- and NLRP3-deficient mice were bred in animal facilities at Johns Hopkins University School of Medicine. All animal experiments were approved by the Institutional Animal Care and Use Committee of the University of California, Davis and performed following the guidelines of Animal Welfare Act and Health Resource Extension Act.

Mouse model of cutaneous infection

Mice were wounded as described previously(5, 6, 20). Briefly, the dorsum of each animal was shaved and the region antiseptically prepared with 10% w/v povidone-iodine and 70% ethanol. A full thickness skin wound was created with a 6 mm dermal punch biopsy and immediately inoculated with 100 μL of sterile saline or S. aureus. Animals were monitored daily until endpoint. Wound area was measured using Living Image 4.3.1 (Caliper Life Science, CA) by drawing circular regions of interest (ROI) over the entire wound. Areas were compared to the initial wound area and expressed as a percentage of closure.

Non-invasive quantification of wound EGFP-PMN

Kinetics of wound EGFP-PMN were quantified on an IVIS Spectrum (PerkinElmer, Waltham, MA) as previously described(5, 6, 20). Briefly, mice were anesthetized by isoflurane gas (2%, inhalation) and placed into the imaging chamber. Wound EGFP signal was visualized using a GFP filter (excitation of 445–490 nm and emission of 515–575 nm)

with an exposure time of 1 second. Images were analyzed using Living Image 4.3.1 and fluorescent intensity was measured over a circular region of interest (ROI) over the entire wound area and expressed as average radiance (photon/s/cm^2/steradian) or total flux (photons/s).

Quantification of bacterial burden

Mice inoculated with wild-type or ΔAT *S. aureus* were euthanized at various time points post inoculation, and excised wound and kidney tissue was homogenized to allow plating of serial dilutions for CFU quantification. In some experiments, S. aureus lux was used to estimate real-time bacterial burden in vivo as previously described(5, 19)

Flow cytometric immunophenotyping

Bone marrow was isolated by crushing 2 femurs in HBSS + 2 mM EDTA + 2% FBS with a mortar and pestle and passed through a 70 μm filter to achieve a single cell suspension. Peripheral blood was drawn into a 1 mL syringe through a 25G needle immediately post-mortem via cardiac puncture. Wounds were collected with an 8 mm dermal punch biopsy, coarsely chopped and enzymatically digested in 20 mM HEPES + Collagenase I (30 mg/mL; Worthington Biochemical Corp., Lakewood, NJ), Collagenase IX (2 mg/mL; Worthington Biochemical Corp.), Neutral Protease (40 mg/mL; Worthington Biochemical Corp.) hyaluronidase (2 mg/mL; Sigma- Aldrich, St. Louis, MO) and DNAse (2 mg/mL; Roche, Basel, Switzerland) for 65 minutes at 37°C, 100 rpm. Wound samples were washed with ice cold PBS + 5 mM EDTA and transferred into fresh tubes through a 70 μm filter. Enzymatic activity was quenched by adding HBSS + 2 mM EDTA +10% FBS to the cell suspension and incubating for 10 minutes at 37°C, 100 rpm. Total number of white blood cells per femur, mL of blood or wound biopsy was determined using an AcT Diff Coulter counter (Beckman Coulter, Indianapolis, IN), and populations of mature PMN (CD11b+, Ly6G+) and progenitor cells (lineage-, ckit-+) were analyzed using FACScan (BD Biosciences, San Jose, CA) and Attune NxT (Thermo Fisher Scientific, Waltham, MA) flow cytometers. The following anti-mouse antibodies were used in this study: Lineage (Pacific Blue, FITC), ckit (APC), Sca-1 (PE), Ly6G (PE, BV421), Mac1 (PE/Cy5), F4/80 (PE), CD45.1 (APC) from Biolegend (San Diego, CA).

In vivo assessment of EGFP-PMN and HSPC trafficking

C57BL/6 recipient mice were wounded and inoculated as described above. Immediately following wounding, BM was collected from LysM-EGFP donor mice and EGFP-PMN were negatively enriched through magnetic separation (Biolegend, San Diego, CA). Analysis by flow cytometry showed enriched samples to be 85–90% pure (EGFP^{hi} Ly6G^{hi} Mac1^{hi}). At 3 hours post wounding, 6×10^6 EGFP-PMN in 100 μL of PBS were intravenously injected into recipient mice via the retro-orbital sinus. To quantify HSPC trafficking efficiency, BM HSPC from C57BL/6 donor mice were enriched by magnetic separation (STEMCELL Technologies, Vancouver, BC) and labeled with VivoTrack680 (PerkinElmer) according to the manufacturer's recommendations. Cells were washed and resuspended at a concentration of 5×10^5 HSPC/100 μL of sterile PBS. At 3 hours post wounding, 5×10^5 labeled HSPC in 100 μL of PBS were intravenously injected into recipient mice via the retro-orbital sinus. PMN or HSPC recruitment efficiency was measured as the

relative EGFP or VivoTrack680 fluorescence intensity at wound sites 24 hours post infusion into S. aureus- versus ΔAT-infected animals compared to saline control. In some experiments, negatively enriched HSPC from LysM-EGFP donor mice were adoptively transferred directly into the wounds of C57BL/6 mice at 3 hours post wounding and inoculation. EGFP-PMN fluorescence was imaged daily on an IVIS Spectrum to track the rate of EGFP- PMN expansion within the wound.

Immunodepletion of PMN and HSPC

PMN and HSPC depletion was performed as described previously(5, 6). Briefly, systemic PMN were depleted by multiple injections of rat anti-mouse anti-Gr-1 monoclonal antibody (RB6-8C5 clone, 0.1 mg each injection; Biolegend). Hematopoietic stem and progenitor cells were depleted by multiple injections of rat anti-mouse anti-ckit monoclonal antibody (ACK2 clone, 1 mg each injection; Biolegend). Control animals were treated with isotype control rat IgG (Biolegend).

In vitro expansion of LSK

BM HSPC from LysM-EGFP mice were enriched by magnetic separation, and 500 lineage negative, c-kit^{+}, SCA-1^{+} cells (LSK) were purified using a MoFlo Astrios cell sorter (Beckman Coulter, Miami, FL) directly into a 96-well plate containing 150 μl base medium (StemSpan SFEM II (STEMCELL Technologies), penicillin, streptomycin, 100 ng/ml SCF (Peprotech Inc., Rocky Hill, NJ), and 100 ng/ml Flt-3L (Peprotech Inc.)) with experimental conditions (500 ng/ml Pam_3CSK_4 (InvivoGen, San Diego, CA); 25 ng/ml IL-1β (Shenendoah Biotechnology Inc., Warwick, PA); 100 ng/ml IL-1RA (Peprotech Inc.)) After 72 hours in culture, 50 μl Sytox Blue (Thermo Fisher Scientific, Waltham, MA) was added and live PMN were enumerated directly on the plate via flow cytometry on an Attune NxT.

LSK inoculation directly into wound bed

LSK cells from unwounded LysM-EGFP, IL-1β$^{-/-}$, or NLRP3$^{-/-}$ donor mice were purified by flow-cytometric cell sorting and cultured for 48 hours in the presence of 500 ng/mL Pam_3CSK_4 to promote TLR2-driven granulopoiesis as previously described(6). At 48 hours, cells were harvested, washed twice in sterile PBS and adjusted to a concentration of 1×10^5 HSPC/100 μL of sterile saline. MyD88-deficient mice were wounded and inoculated with a lethal dose (2e7 CFU) of *S. aureus* lux. At 6 hours post wounding, 100 μL of LysM-EGFP, IL1β$^{-/-}$, or NLRP3$^{-/-}$ HSPC or sterile saline was injected directly into the wound bed. Bacterial bioluminescence and the animals' health were monitored daily until the study endpoint of 14 days.

ELISA for myeloperoxidase (MPO) and IL-1β

Protein levels of MPO (Cayman Chemical, Ann Arbor, MI) and IL-1β (R&D Systems, Minneapolis, MN) were measured ex vivo from homogenized wound tissue according to the manufacturer's recommended instructions.

Live stimulation of mouse PMN with Staphylococcus aureus

PMN were isolated from bone marrow from C57BL/6 mice as described above and stimulated with live *S. aureus* as described previously (21). Briefly, 100,000 PMN were infected with WT *S. aureus* or AT at a MOI of 5:1 in RPMI + 10% FBS for 6 hours at 37°C and 5% CO_2 in a humidified incubator. Gentimicin (20 μg/ml) was added 1 hour into the assay to prevent bacterial overgrowth. At 6 hours media was collected, spun down at 8000 RCF for 10 minutes, and the supernatant collected for an IL-1β ELISA. The caspase1 inhibitor Z-YVAD-FMK (Millipore Inc.) was added at a concentration of 20 μM, and purified alpha-toxin (Sigma Aldrich Inc.) was added at a concentration of 1 μg/ml.

Histopathological evaluation of skin wounds

C57BL/6 mice were wounded and inoculated with sterile saline or 1e7 CFU of WT *S. aureus* or ΔAT. At day 3 post inoculation, animals were euthanized and skin wounds removed with an 8 mm dermal punch biopsy. Samples were bisected along the greatest width of the wound and processed for paraffin embedding and hematoxylin and eosin (H&E) staining. All stained sections were analyzed using a Nikon Eclipse TE2000-U microscope with a 4x objective and a Zyla Image Source color camera. Images were processed using ImageJ (NIH) and Adobe Photoshop software.

Measure of hemolytic activity

Overnight *S. aureus* cultures were spun down at 3300 rpm for 5 min and supernatants filtered through 0.4 μm membranes. Fresh rabbit erythrocytes (Antibodies Inc., Davis, CA) were washed twice and diluted to 2% v/v in sterile PBS. Diluted erythrocytes were co-incubated (1:1 v/v) with serially diluted culture or wound samples at 37°C with 100 rpm agitation for 2 hours. Remaining intact erythrocytes were pelleted and supernatants transferred to a 96-well plate. The amount of hemoglobin release (as a correlate of the extent of hemolysis and total AT activity) was quantified by measuring the absorbance of samples at 405 nm. Values are expressed as the relative hemolytic activity compared to negative (erythrocytes co- incubated with sterile PBS) and positive (erythrocytes co-incubated with 10% Triton-X) controls.

ELISA for alpha-toxin (AT)

96-well microtiter plates (EIA, Costar 9017) containing 100 μL/well of a polyclonal anti-AT antibody (Abcam, ab15948) were incubated overnight at 4°C. The supernatant was removed and wells were blocked with sheep serum (5%, v/v in PBS) for 60 minutes at room temperature. Supernatants were removed and wells washed with 0.05% Tween 20. 100 μl of homogenized wound samples collected at various time points post inoculation with *S. aureus* or ΔAT was added to the wells and incubated for 1 hour at room temperature, followed by three washes with 0.05% Tween 20. 100 μl of anti-AT antibody conjugated to HRP (Abcam, ab15949) diluted 1:300 in 1% sheep serum (v/v) in PBS was added to each well and incubated for 1 hour at room temperature. Supernatants were removed and wells washed with 0.05% Tween 20 followed by PBS. 100 μl of substrate (TMB) was added to each well and the plate was incubated for 10 minutes. 100 μl of stop reagent (2N H2SO4) was added to each well and analyzed immediately on a plate reader at a wavelength of 450 nm.

Adoptive transfer of CD45.1+ HSPC

C57BL/6 (CD45.2+) mice were wounded and inoculated with 1e7 CFU of *S. aureus* versus ΔAT. At 3 hours post wounding, 2×10^6 magnetically enriched HSPC isolated from BM of congenic CD45.1+ donor mice were adoptively transferred directly into wounds. Animals were monitored daily. At day 8 post-wounding, animals were euthanized and wounds collected with an 8 mm dermal punch biopsy. Samples were enzymatically digested and processed for flow cytometry as described previously. Donor-derived PMN expansion was assessed by gating on $CD45.1^+$ progeny.

Statistical analyses

Data analysis was performed using GraphPad Prism version 6.0d (GraphPad Software, San Diego, CA). All data are presented as mean±SEM unless otherwise specified. Differences between single pairs of conditions were analyzed for significance by 2-tailed unpaired Student t-test. Differences between multiple groups were analyzed for significance by 1-way or 2-way ANOVA with Tukey or Dunnett's multiple comparisons posttests. Survival between experimental groups was analyzed for significance by Gehan- Breslow-Wilcoxon test. In some experiments, outliers were identified using Grubb's method. P values < .05 were considered statistically significant.

Results

AT promotes bacterial persistence and subverts immune clearance of *S. aureus*

Neutrophil infiltration and abscess formation are early events in host defense against *S. aureus* skin infections. While previous work demonstrates that AT impairs the host's ability to control *S. aureus* through attenuation of the innate immune response(16, 22), its impact on the dynamics of granulopoiesis, maintenance of PMN numbers and consequent bacterial clearance and wound closure has not been carefully studied. We first examined whether AT affects bacterial burden in LysM-EGFP mice that circulate green fluorescent mature PMN (EGFP-PMN). Mice were wounded and inoculated with saline or 1×10^7 CFU of wild-type (WT) *S. aureus* versus an isogenic AT-deficient mutant (ΔAT). Quantification of CFU recovered from homogenized wound tissue over the course of infection revealed that mice inoculated with WT *S. aureus* maintained a log higher bacterial burden than ΔAT as early as 72 hours post-wounding, and the increased burden was sustained thereafter (Fig. 1A). To longitudinally examine PMN accumulation and its association with bacterial burden at wound sites, *in vivo* whole animal fluorescence imaging was performed. EGFP-PMN accumulated rapidly and to a similar extent over the initial 24 hours in mice inoculated with ΔAT or saline (Fig. 1B). In contrast, mice inoculated with WT *S. aureus* exhibited a ~50% reduction in PMN accumulation, which remained lower than that of ΔAT through day 4. The delay in PMN accumulation in WT *S. aureus* inoculated mice corresponded with significantly delayed wound contraction as compared to mice inoculated with ΔAT or saline (Fig. 1C) and resulted in non-healing wounds that correlated with decreased neutrophilic infiltrates around the wound site (Fig. 1D, Supplemental Fig 1). Assessment of wound tissue homogenates collected at various time points revealed that AT activity and protein levels remained high and correlated with *S. aureus* abundance over time (Supplemental Fig. 2). To confirm the defect in PMN recruitment in WT S. aureus-infected wounds is attributed to AT,

a plasmid of AT was cloned into ΔAT to generate a complement strain (ΔAT-comp). LysM-EGFP mice were wounded and inoculated with 1×10^7 CFU of ΔAT-comp, which resulted in an equivalent defect in recruitment of EGFP-PMN compared with WT *S. aureus* (Supplemental Fig. 2C). Together, these kinetic data demonstrate that AT mediates a persistent delay in PMN accumulation during the inflammatory phase that correlates with increased bacterial persistence and delayed wound resolution.

PMN recruitment to *S. aureus*-infected skin wounds is limited by AT

To investigate whether AT affected the mobilization of mature PMN from the bone marrow (BM) in response to wounding and infection, mice were euthanized at various time points post wounding and PMN numbers in the BM and blood were enumerated by flow cytometry. Wounding alone (saline) resulted in a 25% reduction in BM PMN and an insignificant rise in the frequency of PMN detected in circulation (Fig. 2A and 2B). In contrast, *S. aureus*- and ΔAT-infected animals had a 75% reduction in BM PMN over the initial 24 hours and a compensatory rise in their production by 3 days post inoculation (Fig. 2A). Mice inoculated with WT *S. aureus* maintained ~2 fold greater numbers of PMN in circulation through day 5 compared with ΔAT inoculated mice. Collectively, these data show that AT was responsible for a defective capacity of PMN to be recruited from the circulation to *S. aureus*-infected wounds despite elevated numbers in BM and circulation.

To more directly quantify the efficiency of PMN trafficking to *S. aureus*-infected wounds, mature EGFP-PMN were isolated from the BM of donor LysM-EGFP mice and intravenously transferred into congenic C57BL/6 mice that were previously wounded and inoculated with WT *S. aureus*, ΔAT or saline control. At 24 hours post transfer, detection of EGFP-PMN fluorescence within wounds revealed that ~50% fewer PMN recruited to WT *S. aureus*-inoculated wounds compared with those inoculated with ΔAT or saline (Fig. 2C and 2D). Thus, despite 4-fold greater numbers of circulating PMN, AT mediated a defect in normal recruitment to WT *S. aureus*-infected wounds.

Wounding and infection stimulate HSPC trafficking from bone marrow independent of AT

Next, the influence of AT on HSPC production and trafficking in response to wounding and infection was evaluated. The prevalence of Lin^- $ckit^+$ HSPC within BM and blood samples was analyzed by flow cytometry and revealed that HSPC numbers in BM rose steadily and equivalently in response to WT *S. aureus*, ΔAT or saline (Fig. 3A). Consistent with previous reports, relatively few HSPC (e.g. ~500/mL) were observed in the circulation in response to wounding alone(5). However, by 24 hours post wounding, the number of HSPC increased by 8–10 fold *in S. aureus*- or ΔAT-infected mice compared with saline (Fig. 3B). Circulating numbers of HSPC decreased to an equivalent baseline level among all groups by 3–5 days post wounding (data not shown).

To determine whether the efficiency of HSPC trafficking to wound sites was curtailed by the presence of AT in a manner similar to the recruitment of mature PMN, HSPC from BM of unwounded donor mice were enriched and fluorescently-labeled immediately prior to intravenous infusion into C57BL/6 mice that were wounded and inoculated with WT *S. aureus*, ΔAT or saline (Fig. 3C and 3D). WT *S aureus* elicited a ~25% reduction in HSPC

recruitment efficiency compared with saline, whereas infection with ΔAT did not significantly curtail the trafficking of HSPC. Together, these findings indicate that infection increased the release of HSPC into the circulation, but AT did not impact their trafficking to the site of wounding and infection as observed for PMN recruitment.

Increasing bacterial burden could compensate for reduced granulopoiesis in the setting AT deficiency

To examine the contribution of local granulopoiesis to the rise in PMN numbers detected in *S. aureus*-infected wounds, HSPC isolated from LysM-EGFP mice were adoptively transferred directly into wounds of C57BL/6 mice infected with WT or ΔAT *S. aureus* (Fig. 4A). Wound fluorescence was measured daily in order to gauge the rate of local PMN expansion. Mice inoculated with WT *S. aureus* exhibited a prolonged and steady increase in EGFP-PMN fluorescence through day 8 post infection (Fig. 4B). In contrast, mice inoculated with an equivalent dose of ΔAT exhibited a ~2-fold slower rise in EGFP fluorescence, indicating minimal PMN expansion within the wound (Fig. 4B). To confirm that local granulopoiesis via HSPC accounted for the rise in EGFP-PMN signal, $CD45.1^+$ HSPC were adoptively transferred into wounds of congenic $CD45.2^+$ mice (Supplemental Fig. 3A) and wound homogenates were subsequently collected at day 8 post inoculation for analysis of local expansion of $CD45.1^+$ progeny by flow cytometry (Supplemental Fig. 3B). Consistent with the EGFP-PMN signal, a ~4-fold increase in the number of $CD45.1^+$ PMN were recovered from WT- versus ΔAT-infected $CD45.2^+$ mice (Supplemental Fig. 3C). Remarkably, nearly all $CD45.1^+$ progeny detected in WT-infected wounds were mature PMN ($Ly6G^{hi}$ $Mac1^{hi}$) whereas ΔAT-infected wounds exhibited a heterogeneous population of mature PMN and other $Ly6G^-$ $Mac1^{hi}$ myeloid progeny (Supplemental Fig. 3D). These data suggest that AT was responsible for driving efficient granulopoiesis from HSPC within *S. aureus*-infected wounds.

To determine whether the presence of AT or the concomitant increase in bacterial burden in *S. aureus*-infected mice accounted for the greater local expansion of PMN, mice received repeat inoculations with ΔAT (1×10^7 CFU) at days 2 and 4 post wounding (Fig. 4A). An incremental boost in the rate of PMN expansion was detected with each repeat inoculation, such that three inoculations of ΔAT resulted in an equivalent rate of PMN expansion as WT *S. aureus* (Fig. 4B, 4C). To confirm that repeated inoculation of ΔAT had the intended effect of equalizing bacterial burden, *S. aureus* abundance was measured from homogenized wound tissue samples obtained on day 6 (Fig. 4D). As anticipated, mice inoculated once with WT *S. aureus* maintained significantly higher burden than mice receiving one or two inoculations of ΔAT, whereas ΔATx3 inoculations yielded an equivalent bacterial burden compared to WT infection. We observed that repeat inoculation with ΔAT equalized bacterial burden and promoted a similar degree of PMN expansion as WT *S. aureus*. Therefore, increasing the bacterial burden could compensate for the lack of AT indicating that bacterial burden is an independent determinant that drives local granulopoiesis.

Trafficking and local PMN expansion via HSPC are required for *S. aureus* clearance

Local granulopoiesis within a *S. aureus*-infected abscess accounts for ~30% of total PMN numbers at day 7 post wounding and infection(5, 6). Given that the decrease in *S. aureus*

abundance and wound resolution correlated in time with the latent rise of PMN in WT *S. aureus*-infected mice, we hypothesized that local granulopoiesis played a key role in controlling *S. aureus* infection. To investigate the relative contribution of PMN recruited from the circulation versus those locally expanded from HSPC, LysM-EGFP mice were pre-treated with anti-Gr-1 (αGr-1) monoclonal antibody (mAb) to deplete circulating mature PMN before infecting wounds with WT *S. aureus* or ΔAT. To deplete both mature PMN and HSPC in BM and circulation, αGr-1 was serially injected over five days pre-infection in combination with anti-ckit (αckit) mAb or an isotype control (Fig. 5A) and EGFP-PMN wound fluorescence was quantified daily. A significant proportion (~45%) of the total rate of EGFP-PMN signal rise in response to wounding and *S. aureus* infection remained after PMN depletion (Fig. 5B and 5D). Simultaneous depletion of PMN and HSPC resulted in nearly complete abrogation of the increase in EGFP-PMN, suggesting that local expansion of HSPC played an essential role in providing sufficient PMN to control WT infection. In contrast, wounds inoculated with ΔAT exhibited a greater initial influx but a significantly lower rate of PMN expansion following infection (Fig. 5C and 5D). Combined depletion of PMN and HSPC did not further diminish the rise in signal in response to ΔAT infection. Thus, local expansion of HSPC was promoted by AT and supported the steady increase in PMN in *S. aureus*-infected wounds.

Contribution of IL-1β and TLR2 in promoting HSPC granulopoiesis

AT activates the NLRP3 inflammasome in monocytes, macrophages and PMN, resulting in the processing of pro-IL-1β and secretion of mature IL-1β that can in turn stimulate granulopoiesis in bone marrow (23–25). We next examined the role of AT in production of IL-1β protein in the wounds of mice inoculated with *S. aureus* versus ΔAT. At 24 hours post wounding, a ~2-fold increase was detected for IL-1β protein levels within wounds infected with *S. aureus* compared with ΔAT or saline control (Fig. 6A). To examine whether the deficiency of IL-1β production in wounds was due, in part, to PMN sensing AT and activating the NLRP3 inflammasome, freshly isolated bone marrow derived PMN were stimulated in culture with live *S. aureus*, ΔAT or vehicle control (23). Following 6 hours of stimulation, PMN exposed to *S. aureus* produced ~1-fold more IL-1β compared with ΔAT treatment. Addition of purified AT into the ΔAT culture restored IL-1β production up to levels elicited by *S. aureus*. Moreover, addition of the caspase-1 inhibitor Z-YVAD-FMK abrogated IL-1β production by PMN stimulated by *S. aureus* (Fig. 6B). Together, these data demonstrate that *S. aureus* stimulates PMN in a manner dependent upon NLRP3 inflammasome activity, which is amplified by AT signaling of caspase-1-dependent production of IL-1β.

Signaling via TLR2 or IL-1R can independently promote HSPC proliferation and granulopoiesis (6, 26–29). In addition, our prior work found that TLR2 expressed on the HSPC induced prostaglandin E_2 (PGE2) that acted in an autocrine fashion to promote granulopoiesis (7). Given that the wound environment is rich in bacterial derived TLR2 agonists and PMN derived IL-1β (22), we investigated the combined effect of TLR2 and IL-1R ligation on expansion of lineage negative, c-kit$^+$, SCA-1$^+$ cells (LSK). LSK purified from mouse bone marrow were sorted directly into a 96 well plate and expanded for 72 hours *in vitro* in medium supplemented with a combination of the TLR2 agonist Pam_3CSK_4

and IL-1β. Addition of agonist or cytokine alone induced a 2-fold increase in PMN production, whereas the combination synergistically promoted granulopoiesis as evidenced by a 10-fold increase in expansion compared to vehicle control (Fig 6C). We conclude that TLR2 agonists from gram-positive bacteria and IL-1β from PMN stimulated by AT act synergistically on HSPC to promote PMN expansion.

Local PMN expansion signaled via IL-1β in HSPC rescues MyD88$^{-/-}$ immunodeficient mice from sepsis

Mice lacking MyD88, the signaling adapter downstream of IL-1R/TLR family members, have defective clearance of *S. aureus* skin infections due to impaired PMN recruitment (19, 30). The contribution of IL-1β in promoting local HSPC differentiation and expansion of PMN and their capacity to control cutaneous *S. aureus* infection was evaluated in MyD88$^{-/-}$ mice. LSK cells isolated from LysM-EGFP donor mice were expanded *in vitro* to HSPC in the presence of TLR2 stimulation and injected directly into the wounds of MyD88$^{-/-}$ mice infected with a lethal inoculum of *S. aureus*. Nine of 10 saline-treated MyD88$^{-/-}$ mice succumbed to infection within 7 days post-wounding and infection. In contrast, all of the mice that received injection of HSPC into their wounds survived over the same interval (Fig. 7A). While there was not a measurable difference in bacterial burden between the groups as assessed by *in vivo* bioluminescence imaging, survival in wt HSPC recipients correlated with a significant reduction in bacterial burden in the kidneys by 72 hours post-infection (Fig. 7B, Supplemental Fig. 4), suggesting that HSPC play a critical role in preventing bacterial dissemination. To evaluate whether the local injection of HSPC resulted in an increase in PMN number within *S. aureus*-infected wounds, myeloperoxidase (MPO) levels were measured from homogenized wound tissue collected at 72 hours post-infection. A ~1-fold increase in MPO levels was detected in wt HSPC-treated wounds compared with saline controls (Fig. 7C). Employing MyD88$^{-/-}$ crossbred with LysM-EGFP, we confirmed that the adoptively transferred wt HSPC did not elicit an increase in endogenous PMN recruitment from circulation over the first 3 days of infection (Supplemental Fig. 4B). We conclude that the increase in MPO levels observed in wt HSPC-treated wounds was derived from local expansion of PMN necessary for protection against lethal dissemination of *S. aureus* in MyD88$^{-/-}$ mice.

Next, we investigated whether IL-1β production by HSPC and their PMN progeny was necessary for protection against lethal infection in MyD88$^{-/-}$ mice. HSPC harvested from congenic IL-1β$^{-/-}$ mice were directly delivered to MyD88$^{-/-}$ mice and survival and bacterial burden were monitored over time. IL-1β-deficient HSPC did not improve survival or protection against bacterial dissemination to the kidneys in MyD88$^{-/-}$ mice (Fig. 7A,B). IL-1β$^{-/-}$ HSPC also did not elicit an increase in PMN numbers as indicated by MPO levels that were equivalent to the saline-treated control mice at 72 hours post-infection (Fig. 7C). Correlating with the increase in PMN numbers and survival following transfer of wt HSPC to infected wounds in MyD88$^{-/-}$ mice was a 1-fold greater local production of IL-1β protein compared with the saline or IL-1β$^{-/-}$ HSPC treatments (Fig. 7D). To determine whether NLRP3 inflammasome activity contributed to survival, HSPC collected from the BM of congenic NLRP3$^{-/-}$ mice were injected into wounds of MyD88$^{-/-}$ mice. The survival rate of NLRP3$^{-/-}$ HSPC recipients was intermediate between the WT and the saline or IL-1β$^{-/-}$

HSPC recipients (Supplemental Fig. 4C) Collectively, these data indicate that IL-1β mediated local granulopoiesis by transferred HSPC is necessary for MyD88$^{-/-}$ mice to control a lethal *S. aureus* wound infection, and IL-1β production is in part dependent on NLRP3 inflammasome activity within the progeny of transplanted HSPC.

Discussion

Feedback between the wound and BM is important in regulating appropriate numbers of both PMN and HSPC in circulation and available to recruit to sites of infection. In this report, we demonstrate that AT modulates the host's ability to mount an effective immune response by promoting *S. aureus* colonization and limiting PMN recruitment efficiency into a full-thickness skin wound. Following inoculation with wild-type *S. aureus* versus an isogenic ΔAT mutant, we noted significant attenuation in PMN recruitment from the circulation to wounds inoculated with WT *S. aureus* as compared to ΔAT. Further, we confirmed attenuation in PMN recruitment was restored in a ΔAT-complemented strain that restored *S. aureus* production of AT. A novel finding was that HSPC expanded in BM and trafficked to the site of infection with equal efficiency following inoculation with either strain, signifying that progenitor cell trafficking from BM to wounds is unaffected by AT-mediated toxicity that impedes PMN recruitment. Furthermore, we report that local granulopoiesis and PMN antibacterial defenses play a central role in bacterial clearance and protection from septicemia. The mechanism of local granulopoiesis involved a critical role for TLR2 signaled myeloid differentiation of HSPC and IL-1β driven expansion of mature PMN at the site of infection. Finally, we show that fortifying wounds with exogenously transferred HSPC primed to undergo myeloid expansion effectively rescued MyD88-deficient mice from a lethal wound infection with *S. aureus*.

AT is a clinically important virulence factor that promotes dermonecrosis in *S. aureus* intradermal and subcutaneous infection models in mice(14, 22) through its interaction with A-disintegrin and metalloproteinase 10 (ADAM10) on host cells(31) as well as the adherens junction protein plekstrin-homology domain containing protein 7 (PLEKHA7) expressed by keratinocytes(32). Given its importance in exacerbating infection severity, AT has been a clinical target, employing both monoclonal antibodies and small molecules. These therapies have had a marked effect on reducing disease severity in mouse and rabbit models of *S. aureus* skin infection(33–35). Still, it is unclear whether targeting AT in an active or passive vaccination strategy will be effective as a single antigen, because *S. aureus* produces many other virulence factors that evade host defenses(36). Therefore, we focused our efforts on understanding how AT impacts the neutrophilic response to provide specific host cell mechanisms to target for enhanced clearance of *S. aureus* infections. We found that in a *S. aureus*-infected full-thickness skin wound, AT regulated HSPC recruitment to wounds and PMN expansion at the site of infection through several unexpected observations.

First, circulating PMN were increased 3-fold with WT *S. aureus* compared with infection with the ΔAT mutant or uninfected saline-treated wounds. This was largely due to a reduced capacity of PMN extravasation as evidenced by a 50% reduction in the trafficking efficiency of intravenously transferred PMN. Although the mechanism by which AT led to less PMN extravasation was not directly investigated, a prior report found in a *S. aureus* intradermal

infection model that AT causes lysis and destruction of perivascular macrophages, which lead to a decrease in PMN-attracting chemokines (CXCL1 and CXCL2) and markedly impaired PMN extravasation(16). In contrast to the effect of AT on mature PMN extravasation, AT did not impair the recruitment of HSPC to the site of infection, and the steady rise in EGFP-PMN signal in wounds infected with WT *S. aureus* was instead mediated by local expansion of recruited HSPC. This is consistent with our prior report demonstrating that HSPC numbers can rise 5-fold within a *S. aureus*-infected wound, delivering up to 2×10^5 progenitors at sites of infection, roughly equivalent to the number found in a femur at baseline(6). Underlying differences between AT's influence on the recruitment of PMN versus HSPC to the site of infection is likely due to the chemotactic factors produced in the presence versus absence of AT, as well as differences in the adhesion receptors on mature PMN versus HSPC. For example, CXCL1 and CXCL2 chemokines bind CXCR2 and promote PMN recruitment (37, 38), whereas HSPC express CXCR4 and selectively migrate in response to ligation of CXCL12(39–42). CXCL12 is produced by various cell types in the skin (43, 44), and levels increase in response to wounding (45, 46). A recent report demonstrating that increased production of CXCL12 at wound sites promotes the recruitment of BM-derived mesenchymal stem cells points to a possible mechanism by which CXCL12 may direct HSPC migration to sites of infection as well (47).

Second, we found that there were decreased IL-1β levels in wounds infected with ΔAT compared with WT *S. aureus*, and we observed the same defect *in vitro* by infecting PMN with the wild-type and knockout strains of *S. aureus*. AT is known to be a potent activator of the NLRP3 inflammasome that leads to caspase-1-mediated processing of pro-IL-1β into mature IL-1β (21, 23–25, 48), and mice that harbor a myeloid-specific deletion of ADAM10 suffer exacerbated skin infection that is associated with markedly reduced IL-1β production (49). Likewise, *in vitro*, IL-1β production in PMN cultures stimulated with WT *S. aureus* was abrogated in the presence of a caspase-1 inhibitor, and IL-1β production in PMN cultures stimulated with ΔAT was rescued by addition of purified AT. Taken together, these findings indicate that interaction between AT and ADAM10 on myeloid cells is essential for production of IL-1β, and the decreased levels of IL-1β observed in wounds infected with ΔAT was likely due to a concomitant decrease in NLRP3 inflammasome activation in myeloid cells including PMN, which we reported previously are the most abundant source of IL-1β within a *S. aureus* intradermal infection (23). The results presented here suggest that while AT attenuates the trafficking of mature PMN to wound sites, local detection of AT and activation of the inflammasome is an important host immune tactic to elicit local granulopoiesis. Further, the reduction of IL-1β in ΔAT wounds may also result from a difference in biofilm formation between the two bacterial strains. AT is required for biofilm formation (50) and IL-1β production by PMN is dependent on the size and organization of the microbe it detects (51). Thus the differential response of PMN to the more virulent wt *S. aureus* versus a strain with a defect in biofilm formation, such as ΔAT, could account for diminished cytokine production.

A third key finding was the synergistic role of TLR2 and IL-1β signaling in inducing local granulopoiesis of the recruited HSPC. This is significant because *S. aureus* possesses TLR2 ligands, particularly lipopeptides and lipoteichoic acid in its cell wall, and both TLR2 and IL-1R can promote HSPC proliferation and granulopoiesis in other model systems (6, 26–

29, 50). However, their cooperative contribution to local granulopoiesis in the context of *S. aureus*-infected wounds had not been reported. We found that in response to *in vitro* stimulation with the TLR2 agonist, Pam_3CSK_4, and recombinant IL-1β there was a 100% increase in granulopoiesis compared to either stimulus alone. The novel finding here was that neutrophil-derived IL-1β and *S. aureus*-stimulated TLR2 signaling act synergistically and in part through the inflammasome to promote expansion of PMN from HSPC. We previously found that TLR2/MyD88 activation on HSPCs led to PGE_2 production that provided an autocrine signal to promote granulopoiesis (7). It is tempting to speculate that IL-1β acts in a similar manner in promotion of HSPC differentiation and this will be a subject for future work.

Finally, our data demonstrate that IL-1β signaling drives local granulopoiesis, but the source of IL-1β and involvement of autocrine versus paracrine activation of HSPC remains ill-defined. Taking into account our finding of a doubling in MPO levels that correlated closely with increased PMN numbers and concomitant local production of IL-1β following adoptive transfer of wild-type but not IL-1β$^{-/-}$ HSPC, we surmise that local granulopoiesis is promoted by autocrine IL-1β production. While it is possible that other IL-1β-producing cells promote local granulopoiesis through paracrine signaling, we previously reported defective local granulopoiesis from HSPC derived from MyD88$^{-/-}$ donor mice that were adoptively transferred into the wounds of infected wt mice(6). Several mechanisms of IL-1β production may be involved in the wounds. The survival of MyD88$^{-/-}$ mice depended on IL-1β in the transferred HSPC, and mice receiving NLRP3$^{-/-}$ HSPC faired worse than those receiving wt HSPC, This indicates that the NLRP3/caspase-1 inflammasome is in part responsible for the survival conferred by the cells and that inflammasome-independent mechanisms of IL-1β production may also contribute to the improved survival observed in our model. Neutrophil derived proteinase-3 and pathogen derived proteases are both capable of processing pro-IL-1β to IL-1β in neutrophils (53, 54), and future studies are required to determine their relative contributions to IL-1β production in *S. aureus* infection. Taken together, we propose that IL-1β produced by HSPC's expanding progeny induce myeloid differentiation and significantly expand PMN numbers through autocrine feedback signaling. It is likely that IL-1β plays a similar role in promoting local granulopoiesis in other tissues infected with *S. aureus*. In particular, AT-induced IL-1β production promotes excessive PMN infiltration and exacerbation of pneumonia during *S. aureus* pulmonary infections (49). Future studies will determine whether *S. aureus* induced HSPC recruitment and local granulopoiesis are involved in *S. aureus* pneumonia and at other sites of tissue infection.

In conclusion, trafficking and local myeloid expansion of HSPC at the site of *S. aureus*-infected wounds provides a host immune tactic for circumvention of acute neutropenia mediated by AT, a key virulence factor employed by *S. aureus*. These findings support a strategy of active or passive vaccination approaches that target AT. However, *S. aureus* produces many other virulence factors that evade host defense mechanisms and it is important to consider alternate strategies that fortify innate immune mechanisms for bacterial clearance. A strategy in which TLR2 and IL-1β are used to prime autologous HSPC to expand PMN on demand may provide an immune-based alternative and/or complementary therapeutic approach to combat *S. aureus*-infected wounds, which might be

especially relevant for infections caused by virulent and multi-drug resistant MRSA strains or in immunocompromised individuals.

Supplementary Material

Refer to Web version on PubMed Central for supplementary material.

Acknowledgments

This work was supported by grants from the National Institute of Health, (R01 AI047294 to S.I.S.; R56 AI103687 to S.I.S.; and R01 AR069502 to L.S.M.), the Howard Hughes Medical Institute's Integrating Medicine into Basic Science Training Program at UC Davis (56006769 to P.C.F.), and the Training Program in Pharmacology: From Bench to Bedside at UC Davis (NIH T32 GM099608 to L.S.A)

References

1. Schierle CF, De la Garza M, Mustoe TA, Galiano RD. Staphylococcal biofilms impair wound healing by delaying reepithelialization in a murine cutaneous wound model. Wound Repair and Regeneration. 2009; 17:354–359. [PubMed: 19660043]
2. Gordon RJ, Lowy FD. Pathogenesis of Methicillin-Resistant Staphylococcus aureus Infection. Clin Infect Dis. 2008; 46:S350–S359. [PubMed: 18462090]
3. Miller LS, Cho JS. Immunity against Staphylococcus aureus cutaneous infections. Nature Reviews Immunology. 2011; 11:505–518.
4. Mölne L, Verdrengh M, Tarkowski A. Role of Neutrophil Leukocytes in Cutaneous Infection Caused by Staphylococcus aureus. Infect. Immun. 2000; 68:6162–6167. [PubMed: 11035720]
5. Kim MH, Granick JL, Kwok C, Walker NJ, Borjesson DL, Curry FRE, Miller LS, Simon SI. Neutrophil survival and c-kit+-progenitor proliferation in Staphylococcus aureus-infected skin wounds promote resolution. Blood. 2011; 117:3343–3352. [PubMed: 21278352]
6. Granick JL, Falahee PC, Dahmubed D, Borjesson DL, Miller LS, Simon SI. Staphylococcus aureus recognition by hematopoietic stem and progenitor cells via TLR2/MyD88/PGE2 stimulates granulopoiesis in wounds. Blood. 2013; 122:1770–1778. [PubMed: 23869087]
7. Foster TJ. Immune evasion by staphylococci. Nature Reviews Microbiology. 2005; 3:948–958. [PubMed: 16322743]
8. Rooijakkers SHM, van Kessel KPM, van Strijp JAG. Staphylococcal innate immune evasion. Trends in Microbiology. 2005; 13:596–601. [PubMed: 16242332]
9. Rigby KM, DeLeo FR. Neutrophils in innate host defense against Staphylococcus aureus infections. Semin Immunopathol. 2012; 34:237–259. [PubMed: 22080185]
10. Kobayashi SD, Malachowa N, DeLeo FR. Pathogenesis of Staphylococcus aureus Abscesses. The American Journal of Pathology. 2015; 185:1518–1527. [PubMed: 25749135]
11. Berube B, Wardenburg J. Staphylococcus aureus α-Toxin: Nearly a Century of Intrigue. Toxins 2013, Vol 5, Pages 1140-1166. 2013; 5:1140–1166.
12. Wardenburg JB, Bae T, Otto M, DeLeo FR, Schneewind O. Poring over pores: |[alpha]|-hemolysin and Panton-Valentine leukocidin in Staphylococcus aureus pneumonia. Nature Medicine. 2007; 13:1405–1406.
13. Wardenburg JB, Schneewind O. Vaccine protection against Staphylococcus aureus pneumonia. J Exp Med. 2008; 205:287–294. [PubMed: 18268041]
14. Kennedy AD, Wardenburg JB, Gardner DJ, Long D, Whitney AR, Braughton KR, Schneewind O, DeLeo FR. Targeting of Alpha-Hemolysin by Active or Passive Immunization Decreases Severity of USA300 Skin Infection in a Mouse Model. J Infect Dis. 2010; 202:1050–1058. [PubMed: 20726702]
15. Brady RA, Mocca CP, Prabhakara R, Plaut RD, Shirtliff ME, Merkel TJ, Burns DL. Evaluation of Genetically Inactivated Alpha Toxin for Protection in Multiple Mouse Models of Staphylococcus aureus Infection. PLoS ONE. 2013; 8:e63040. [PubMed: 23658662]

16. Abtin A, Jain R, Mitchell AJ, Roediger B, Brzoska AJ, Tikoo S, Cheng Q, Ng LG, Cavanagh LL, von Andrian UH, Hickey MJ, Firth N, Weninger W. Perivascular macrophages mediate neutrophil recruitment during bacterial skin infection. Nature Immunology. 2013; 15:45–53. [PubMed: 24270515]

17. Tkaczyk C, Hua L, Varkey R, Shi Y, Dettinger L, Woods R, Barnes A, MacGill RS, Wilson S, Chowdhury P, Stover CK, Sellman BR. Identification of Anti-Alpha Toxin Monoclonal Antibodies That Reduce the Severity of Staphylococcus aureus Dermonecrosis and Exhibit a Correlation between Affinity and Potency. Clin. Vaccine Immunol. 2012; 19:377–385. [PubMed: 22237895]

18. Horsburgh MJ, Aish JL, White IJ, Les Shaw Lithgow JK, Foster SJ. σB Modulates Virulence Determinant Expression and Stress Resistance: Characterization of a Functional rsbU Strain Derived from Staphylococcus aureus 8325-4. J. Bacteriol. 2002; 184:5457–5467. [PubMed: 12218034]

19. Miller LS, O'Connell RM, Gutierrez MA, Pietras EM, Shahangian A, Gross CE, Thirumala A, Cheung AL, Cheng G, Modlin RL. MyD88 Mediates Neutrophil Recruitment Initiated by IL-1R but Not TLR2 Activation in Immunity against Staphylococcus aureus. Immunity. 2006; 24:79–91. [PubMed: 16413925]

20. Kim M-H, Liu W, Borjesson DL, Curry F-RE, Miller LS, Cheung AL, Liu F-T, Isseroff RR, Simon SI. Dynamics of Neutrophil Infiltration during Cutaneous Wound Healing and Infection Using Fluorescence Imaging. Journal of Investigative Dermatology. 2008; 128:1812–1820. [PubMed: 18185533]

21. Mariathasan S, Weiss DS, Newton K, McBride J, O'Rourke K, Roose-Girma M, Lee WP, Weinrauch Y, Monack DM, Dixit VM. Cryopyrin activates the inflammasome in response to toxins and ATP. Nature. 2006; 440:228–232. [PubMed: 16407890]

22. Tkaczyk C, Hamilton MM, Datta V, Yang XP, Hilliard JJ, Stephens GL, Sadowska A, Hua L, O'Day T, Suzich J, Stover CK, Sellman BR. Staphylococcus aureus Alpha Toxin Suppresses Effective Innate and Adaptive Immune Responses in a Murine Dermonecrosis Model. PLoS ONE. 2013; 8:e75103. [PubMed: 24098366]

23. Cho JS, Guo Y, Ramos RI, Hebroni F, Plaisier SB, Xuan C, Granick JL, Matsushima H, Takashima A, Iwakura Y, Cheung AL, Cheng G, Lee DJ, Simon SI, Miller LS. Neutrophil-derived IL-1β Is Sufficient for Abscess Formation in Immunity against Staphylococcus aureus in Mice. PLoS Pathog. 2012; 8:e1003047. [PubMed: 23209417]

24. Craven RR, Gao X, Allen IC, Gris D, Wardenburg JB, McElvania-TeKippe E, Ting JP, Duncan JA. Staphylococcus aureus α-Hemolysin Activates the NLRP3-Inflammasome in Human and Mouse Monocytic Cells. PLoS ONE. 2009; 4:e7446. [PubMed: 19826485]

25. Muñoz-Planillo R, Franchi L, Miller LS, Núñez G. A Critical Role for Hemolysins and Bacterial Lipoproteins in Staphylococcus aureus-Induced Activation of the Nlrp3 Inflammasome. The Journal of Immunology. 2009; 183:3942–3948. [PubMed: 19717510]

26. Granick JL, Simon SI, Borjesson DL. Hematopoietic Stem and Progenitor Cells as Effectors in Innate Immunity. Bone Marrow Research. 2012; 2012:1–8.

27. Nagai Y, Garrett KP, Ohta S, Bahrun U, Kouro T, Akira S, Takatsu K, Kincade PW. Toll-like Receptors on Hematopoietic Progenitor Cells Stimulate Innate Immune System Replenishment. Immunity. 2006; 24:801–812. [PubMed: 16782035]

28. Ueda Y, Cain DW, Kuraoka M, Kondo M, Kelsoe G. IL-1R Type I-Dependent Hemopoietic Stem Cell Proliferation Is Necessary for Inflammatory Granulopoiesis and Reactive Neutrophilia. The Journal of Immunology. 2009; 182:6477–6484. [PubMed: 19414802]

29. Pietras EM, Mirantes-Barbeito C, Fong S, Loeffler D, Kovtonyuk LV, Zhang S, Lakshminarasimhan R, Chin CP, Techner J-M, Will B, Nerlov C, Steidl U, Manz MG, Schroeder T, Passegué E. Chronic interleukin-1 exposure drives haematopoietic stem cells towards precocious myeloid differentiation at the expense of self-renewal. Nature Cell Biology. 2016; 18:607–618. [PubMed: 27111842]

30. Feuerstein R, Seidl M, Prinz M, Henneke P. MyD88 in Macrophages Is Critical for Abscess Resolution in Staphylococcal Skin Infection. The Journal of Immunology. 2015; 194:2735–2745. [PubMed: 25681348]

31. Inoshima N, Wang Y, Wardenburg JB. Genetic Requirement for ADAM10 in Severe Staphylococcus aureus Skin Infection. The Journal of investigative dermatology. 2012; 132:1513–1516. [PubMed: 22377761]
32. Popov LM, Marceau CD, Starkl PM, Lumb JH, Shah J, Guerrera D, Cooper RL, Merakou C, Bouley DM, Meng W, Kiyonari H, Takeichi M, Galli SJ, Bagnoli F, Citi S, Carette JE, Amieva MR. The adherens junctions control susceptibility to Staphylococcus aureus α-toxin. PNAS. 2015; 112:14337–14342. [PubMed: 26489655]
33. Sampedro GR, DeDent AC, Becker REN, Berube BJ, Gebhardt MJ, Cao H, Wardenburg JB. Targeting Staphylococcus aureus α-Toxin as a Novel Approach to Reduce Severity of Recurrent Skin and Soft-Tissue Infections. J Infect Dis. 2014; 210:1012–1018. [PubMed: 24740631]
34. Hilliard JJ, Datta V, Tkaczyk C, Hamilton M, Sadowska A, Jones-Nelson O, O'Day T, Weiss WJ, Szarka S, Nguyen V, Prokai L, Suzich J, Stover CK, Sellman BR. Anti-Alpha-Toxin Monoclonal Antibody and Antibiotic Combination Therapy Improves Disease Outcome and Accelerates Healing in a Staphylococcus aureus Dermonecrosis Model. Antimicrob. Agents Chemother. 2015; 59:299–309. [PubMed: 25348518]
35. Le TVM, Tkaczyk C, Chau S, Rao RL, Dip EC, Pereira-Franchi EP, Cheng L, Lee S, Koelkebeck H, Hilliard JJ, Yu XQ, Datta V, Nguyen V, Weiss W, Prokai L, O'Day T, Stover CK, Sellman BR, Diep BA. Critical Role of Alpha-Toxin and Protective Effects of Its Neutralization by a Human Antibody in Acute Bacterial Skin and Skin Structure Infections. Antimicrob. Agents Chemother. 2016; 60:5640–5648. [PubMed: 27401576]
36. Spaan, AN., Surewaard, BGJ., Nijland, R., van Strijp, JAG. Neutrophils Versus Staphylococcus aureus: A Biological Tug of War*. 2013. http://dx.doi.org/10.1146/annurev-micro-092412-155746
37. Williams MR, Azcutia V, Newton G, Alcaide P, Luscinskas FW. Emerging mechanisms of neutrophil recruitment across endothelium. Trends in Immunology. 2011; 32:461–469. [PubMed: 21839681]
38. Kolaczkowska E, Kubes P. Neutrophil recruitment and function in health and inflammation. Nature Reviews Immunology. 2013; 13:159–175.
39. Wright DE, Bowman EP, Wagers AJ, Butcher EC, Weissman IL. Hematopoietic Stem Cells Are Uniquely Selective in Their Migratory Response to Chemokines. J Exp Med. 2002; 195:1145–1154. [PubMed: 11994419]
40. Ceradini DJ, Kulkarni AR, Callaghan MJ, Tepper OM, Bastidas N, Kleinman ME, Capla JM, Galiano RD, Levine JP, Gurtner GC. Progenitor cell trafficking is regulated by hypoxic gradients through HIF-1 induction of SDF-1. Nature Medicine. 2004; 10:858–864.
41. Massberg S, von Andrian UH. Novel Trafficking Routes for Hematopoietic Stem and Progenitor Cells. Annals of the New York Academy of Sciences. 2009; 1176:87–93. [PubMed: 19796236]
42. Mazo IB, Massberg S, von Andrian UH. Hematopoietic stem and progenitor cell trafficking. Trends in Immunology. 2011; 32:493–503. [PubMed: 21802990]
43. Pablos JL, Amara A, Bouloc A, Santiago B, Caruz A, Galindo M, Delaunay T, Virelizier JL, Arenzana-Seisdedos F. Stromal-Cell Derived Factor Is Expressed by Dendritic Cells and Endothelium in Human Skin. The American Journal of Pathology. 1999; 155:1577–1586. [PubMed: 10550315]
44. Avniel S, Arik Z, Maly A, Sagie A, Basst HB, Yahana MD, Weiss ID, Pal B, Wald O, Ad-El D, Fujii N, Arenzana-Seisdedos F, Jung S, Galun E, Gur E, Peled A. Involvement of the CXCL12/CXCR4 Pathway in the Recovery of Skin Following Burns. Journal of Investigative Dermatology. 2006; 126:468–476. [PubMed: 16385346]
45. Toksoy A, Müller V, Gillitzer R, Goebeler M. Biphasic expression of stromal cell-derived factor-1 during human wound healing. British Journal of Dermatology. 2007; 157:1148–1154. [PubMed: 17941943]
46. Sun J, Nemoto E, Hong G, Sasaki K. Modulation of stromal cell-derived factor 1 alpha (SDF-1α) and its receptor CXCR4 in Porphyromonas gingivalis- induced periodontal inflammation. BMC Oral Health 2016 17:1. 2016; 17:26.
47. Xu X, Zhu F, Zhang M, Zeng D, Luo D, Liu G, Cui W, Wang S, Guo W, Xing W, Liang H, Li L, Fu X, Jiang J, Huang H. Stromal Cell-Derived Factor-1 Enhances Wound Healing through

Recruiting Bone Marrow-Derived Mesenchymal Stem Cells to the Wound Area and Promoting Neovascularization. CTO. 2013; 197:103–113. [PubMed: 23207453]

48. Kebaier C, Chamberland RR, Allen IC, Gao X, Broglie PM, Hall JD, Jania C, Doerschuk CM, Tilley SL, Duncan JA. Staphylococcus aureus α-Hemolysin Mediates Virulence in a Murine Model of Severe Pneumonia Through Activation of the NLRP3 Inflammasome. J Infect Dis. 2012; 205:807–817. [PubMed: 22279123]
49. Becker REN, Berube BJ, Sampedro GR, DeDent AC, Bubeck Wardenburg J. Tissue-Specific Patterning of Host Innate Immune Responses by Staphylococcus aureus α-Toxin. J Innate Immun. 2014; 6:619–631. [PubMed: 24820433]
50. De Luca K, Frances-Duvert V, Asensio M-J, Ihsani R, Debien E, Taillardet M, Verhoeyen E, Bella C, Lantheaume S, Genestier L, Defrance T. The TLR1/2 agonist PAM3CSK4 instructs commitment of human hematopoietic stem cells to a myeloid cell fate. Leukemia. 2009; 23:2063–2074. [PubMed: 19641520]

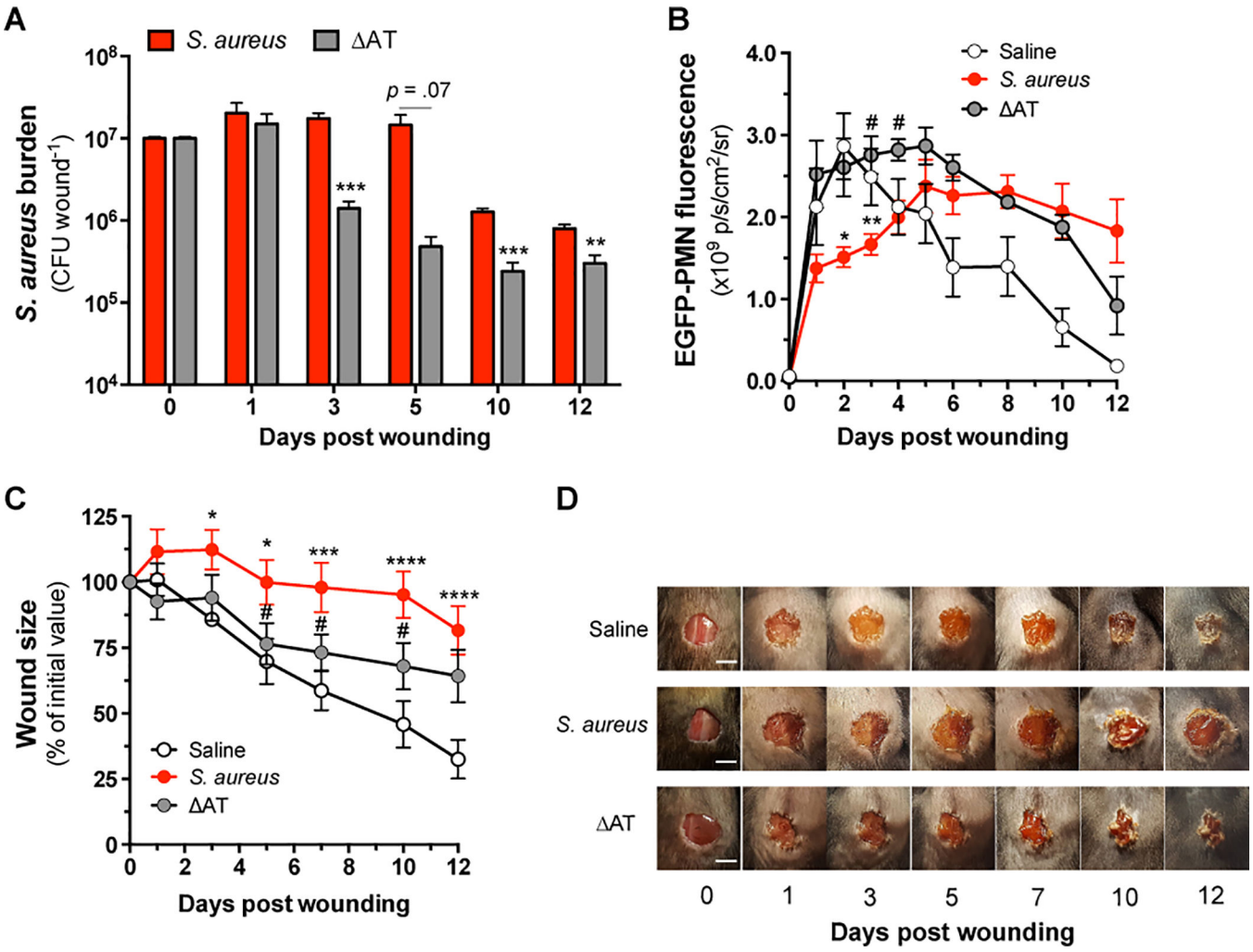

Figure 1. Alpha-toxin sustains *S. aureus* burden and delays PMN accumulation and wound healing

LysM-EGFP mice were wounded and inoculated with saline or 1×10^7 CFU of *S. aureus* or the isogenic AT-deficient mutant (ΔAT). (A) Kinetics of *S. aureus* burden measured from tissue homogenates collected after wounding and inoculation at day 0. (B) EGFP-PMN fluorescence measured at wound sites. (C) Wound size relative to the initial area of 6 mm. (D) Representative wound images are shown for each treatment group. Scale bars = 5 mm. Data are derived from 3–11 mice per group and are expressed as mean±SEM. * $p < .05$, ** $p < .01$, *** $p < .001$, *S. aureus* or ΔAT versus saline control. # $p < .05$, *S. aureus* versus ΔAT. 1A: two-tailed unpaired *t* test; 1B-C: 2-way ANOVA ($p < .0001$ for each) with Tukey's multiple comparisons test.

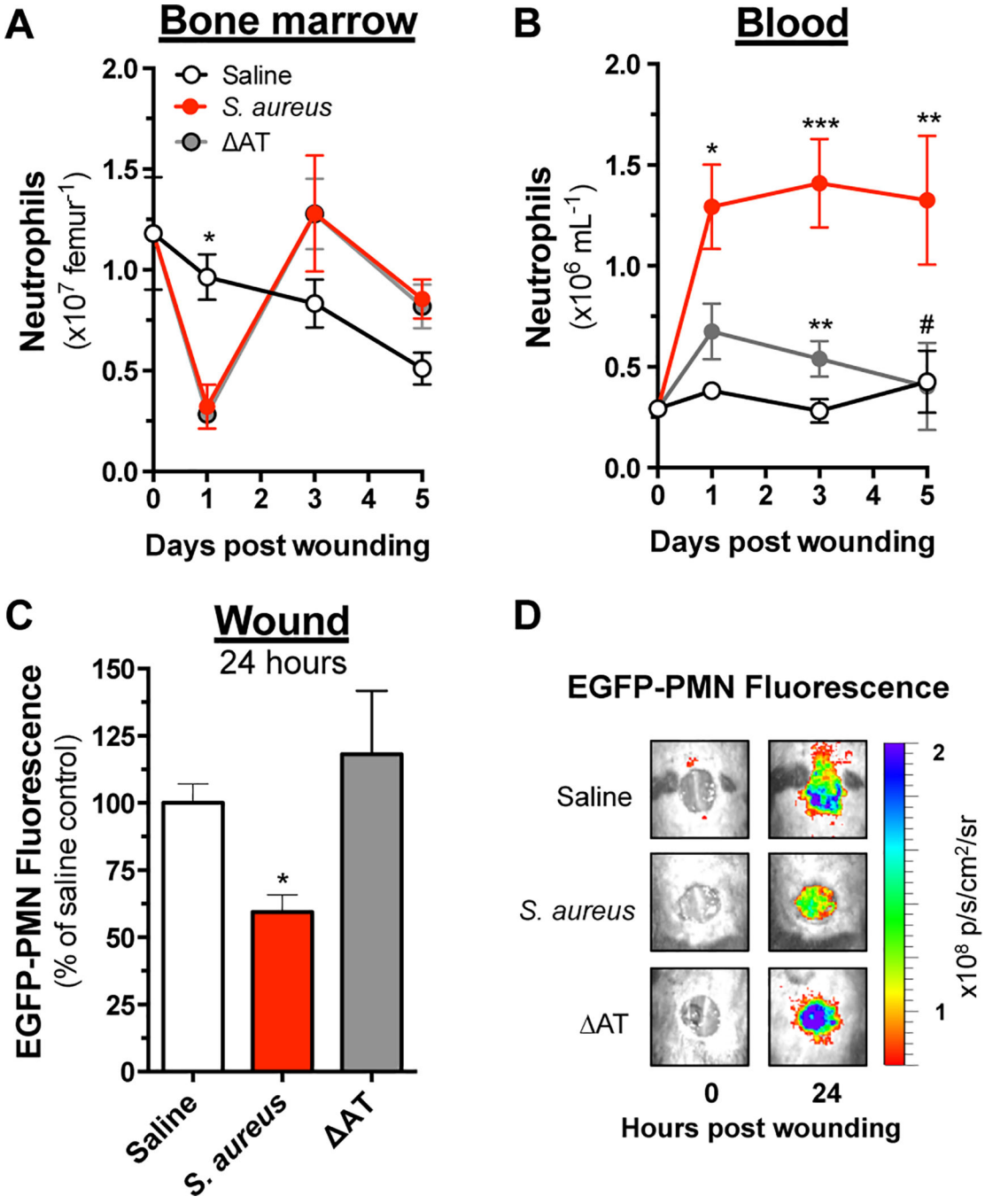

Figure 2. Alpha-toxin disrupts trafficking of PMN from bone marrow into a *S. aureus* infected wound

C57BL/6 mice were wounded and inoculated with saline or 1×10^7 CFU of *S. aureus* versus ΔAT. Mice were euthanized at various endpoints and the number of $Ly6G^{hi}$ $Mac1^{hi}$ PMN in (A) bone marrow and (B) peripheral blood was determined by flow cytometry. (C) Separate cohorts of dark mice received 6×10^6 EGFP-PMN via intravenous transfer 3 hours after wounding and inoculation, and the relative recruitment was determined based on the total EGFP fluorescence at wound sites 24 hours later. (D) Representative images showing PMN fluorescence at wound sites immediately following wounding and 24 hours later are shown.

Data represent 3–10 mice per group and are expressed as mean±SEM. * $p < .05$, ** $p < .01$, *** $p < .001$, *S. aureus* or ΔAT versus saline control. # $p < .05$, *S. aureus* versus ΔAT. 2-way ANOVA ($p < .05$ and $p < .01$ for 2A and 2B, respectively) with Tukey's multiple comparisons test. 2C: 1-way ANOVA (2C, $p < .05$) with Tukey's multiple comparisons test.

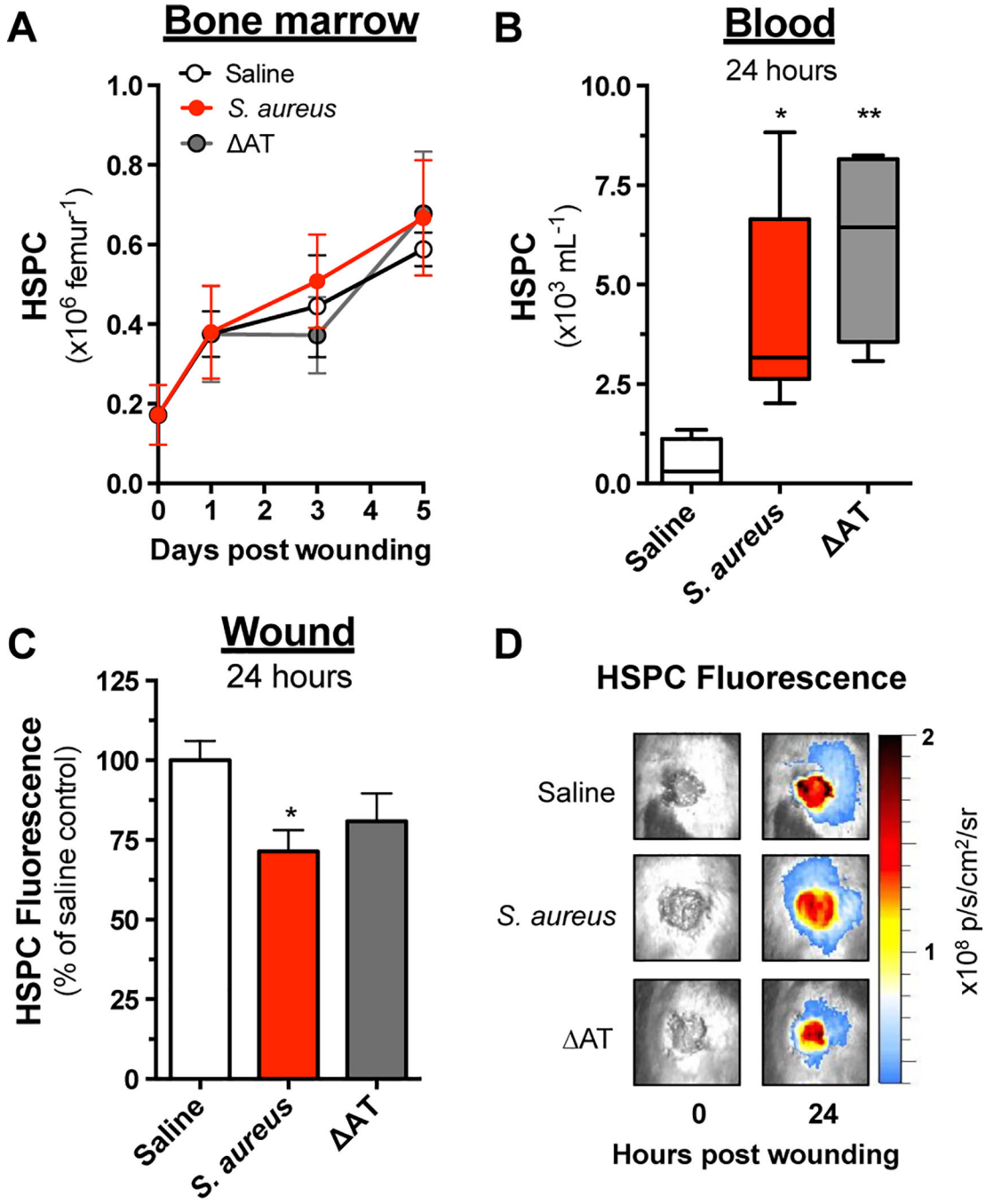

Figure 3. HSPC trafficking is not affected by AT-mediated toxicity

Wounded C57BL/6 mice were euthanized at various endpoints following inoculation with sterile saline or 1×10^7 CFU of *S. aureus* versus ΔAT, and the prevalence of Lin ckit$^+$ HSPC in (A) bone marrow and (B) peripheral blood was determined by flow cytometry. (C) Separate cohorts of mice received 5×10^5 fluorescently labeled HSPC via intravenous transfer 3 hours after wounding and inoculation, and relative recruitment was determined based on the total fluorescence signal at wound sites 24 hours later. (D) Representative images showing HSPC fluorescence at wound sites immediately following wounding and 24

hours later are shown. Data represent 4–7 mice per group and are expressed as mean±SEM. * $p < .05$, ** $p < .01$, *S. aureus* or ΔAT versus saline. 1-way ANOVA ($p < .01$ and $p < .05$ for 3B and 3C, respectively) with Tukey's multiple comparisons test.

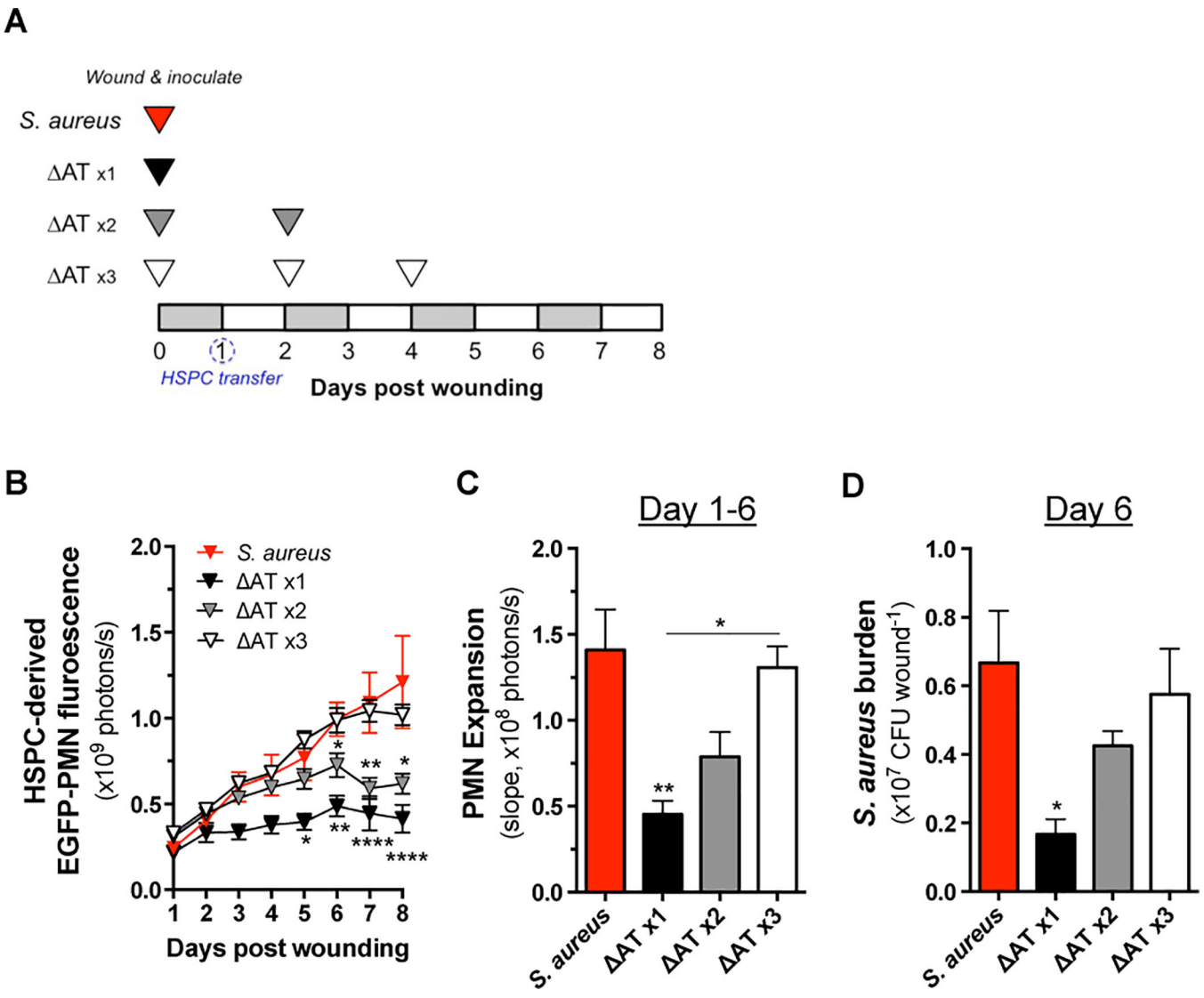

Figure 4. HSPC expansion within the wound is responsive to bacterial abundance

(A) C57BL/6 mice were wounded and inoculated with 1×10^7 CFU of *S. aureus* or ΔAT. At 24 hours post wounding, mice received a local injection of 5×10^5 HSPC from LysM-EGFP donor mice. Some animals that received ΔAT at day 0 received additional inoculations of equivalent CFU at day 2 or days 2 and 4 post wounding as indicated. (B) EGFP-PMN fluorescence at wound sites was quantified daily. (C) The rate of increasing EGFP-PMN fluorescence was determined based on the slopes depicted in panel B. (D) Bacterial burden from wounds of mice from each experimental group was determined from homogenized wound tissue collected at day 6 post wounding. Data represent 4–10 mice per group and are expressed as mean±SEM. * $p < .05$, ** $p < .01$, versus *S. aureus* or as indicated. 1-way ANOVA ($p < .01$ and $p < .01$ for 4B and 4C, respectively) with Tukey's multiple comparisons test. 1-way ANOVA (4D, ns) with Dunnett's multiple comparisons test.

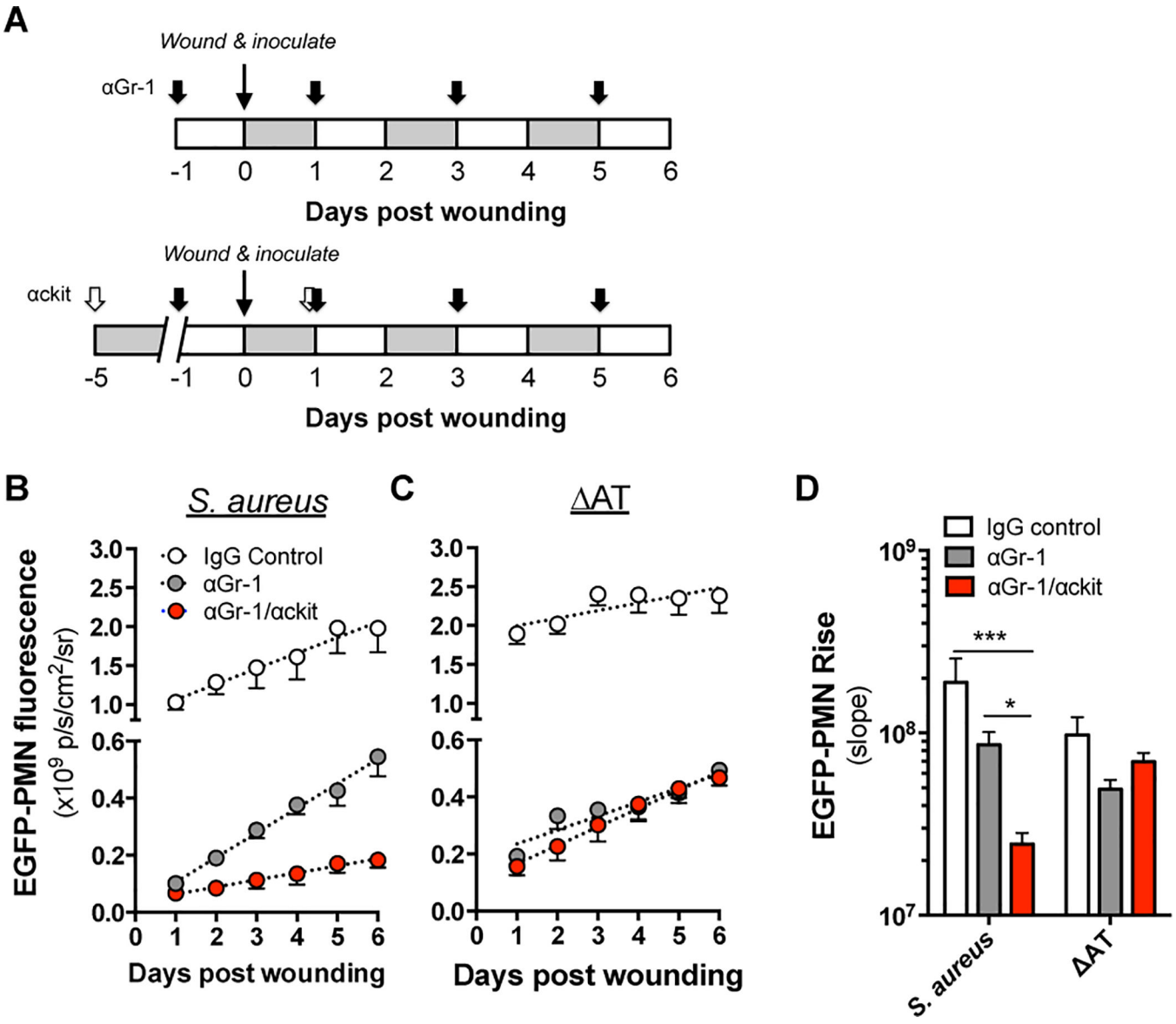

Figure 5. Local granulopoiesis provides a significant source of PMN in *S. aureus* infected wounds

(A) Monoclonal antibodies were administered via intraperitoneal injection to block trafficking of PMN (αGr-1) or PMN and HSPC (αGr-1/αckit) to wounded LysM-EGFP mice according to the experimental design depicted. Wound fluorescence was quantified daily for each group in response to 1e7 CFU of (B) *S. aureus* or (C) ΔAT. (D) The relative rate of EGFP-PMN expansion was compared between treatment groups. Data represent 4–6 mice per group and are expressed as mean±SEM. * $p < .05$, *** $p < .001$, as indicated. 1-way ANOVA ($p < .0001$ for 5B and 5D) with Dunnett's multiple comparisons test.

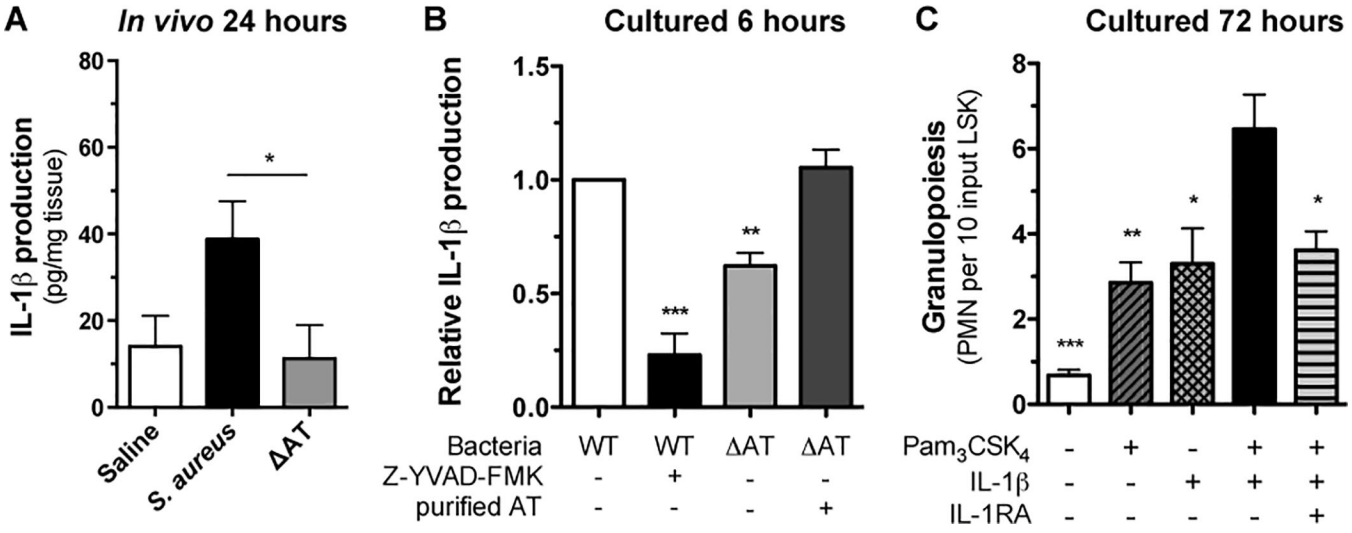

Figure 6. IL-1β and TLR2 activation signals granulopoiesis of bone marrow derived HSPC

(A) IL-1β protein expression from homogenized wound tissue collected 24 hours post wounding and inoculation with saline or *S. aureus* versus ΔAT as measured by ELISA. (B) Bone marrow derived PMN were stimulated with live *S. aureus* or ΔAT in the presence and absence of a caspase1 inhibitor (Z-YVAD-FMK) and purified alpha-toxin. IL-1β protein levels were measured in culture supernatants by ELISA. Non-stimulated cells showed protein levels below the limit of detection for the ELISA (data not shown). Data normalized for each mouse to IL-1β produced by WT *S. aureus*. (C) *In vitro* expansion of LSK from BM-derived HSPC cultured for 72 hours with Pam_3CSK_4 alone, IL-1β alone, Pam_3CSK_4 + IL-1β, Pam_3CSK_4 + IL-1β + IL-1RA, or vehicle control. Data are expressed as mean±SEM and represent at least 3 independent experiments. * $p < .05$, ** $p < .01$, *** $p < .001$, WT + Z-YVAD-FMK, ΔAT, or ΔAT + AT versus WT alone (B) or vehicle, Pam_3CSK_4 alone, IL-1β alone, or Pam_3CSK_4 + IL-1β + IL-1RA versus Pam_3CSK_4 + IL-1β (C). 6A: two-tailed unpaired t-test; 6B-C: 1-way ANOVA ($p<0.0001$ for 6B and 6C) with Tukey's multiple comparisons test.

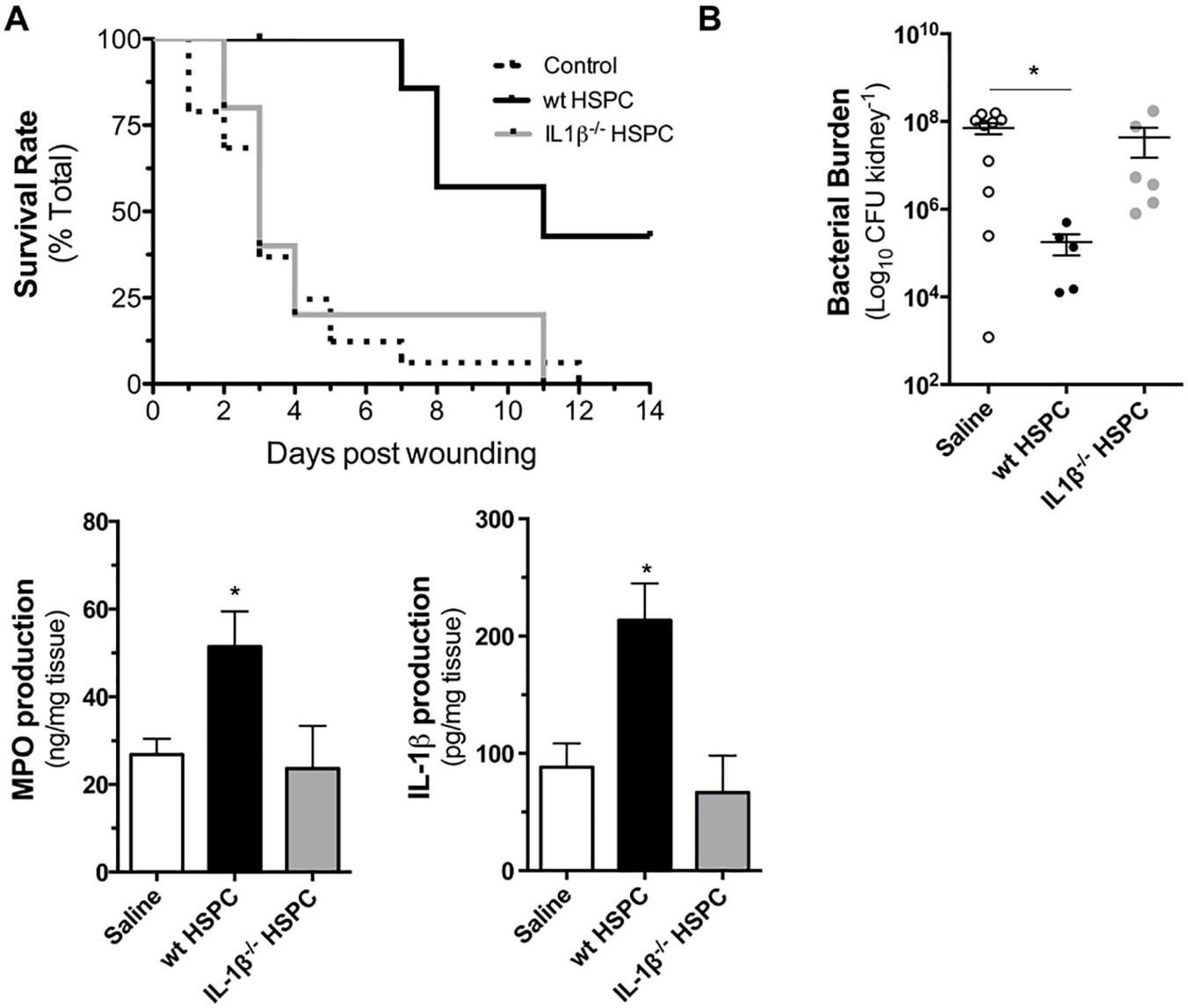

Figure 7. Adoptive transfer of HSPC confers protection from lethal *S. aureus* infection in MyD88$^{-/-}$ mice in an IL-1β-dependent manner

MyD88$^{-/-}$ mice were wounded and infected with a lethal dose of 2e7 CFU of bioluminescent *S. aureus*. At 6 hours post inoculation, wounds were injected with either 1×10^5 HSPC derived from the bone marrow of wild-type (wt) or IL-1β$^{-/-}$ mice or vehicle control. (A) Kaplan-Meier survival plots are shown. Separate cohorts of mice were euthanized at 72 hours post wounding and inoculation and (B) bacterial burden in the kidneys, (C) MPO and (D) IL-1β were quantified from homogenized tissue samples. Data represent 5–10 mice per group and are expressed as mean±SEM. * $p < .05$, ** $p < .01$, *** p < .001 compared to saline control or as indicated. Gehan-Breslow-Wilcoxon test (7A); 1-way ANOVA ($p < .05$, $p < .05$ and $p < .01$ for 7B, 7C and 7D, respectively) with Tukey's multiple comparisons test.